Polymer chain in a random array of topological obstacles: Classification and statistics of complex loops

V. G. Rostiashvili
Max-Planck-Institut für Polymerforschung, Postfach 3148, D-W-6500 Mainz, Federal Republic of Germany

S. K. Nechaev
L.D. Landau Institute for Theoretical Physics, 117940 Moscow, Russia

T. A. Vilgis
Max-Planck-Institut für Polymerforschung, Postfach 3148, D-W-6500 Mainz, Federal Republic of Germany
(Received 20 November 1992)

An arbitrary complex polymer loop embedded in three-dimensional space and topologically entangled with a quenched array of randomly dstributed parallel rods is considered. It is shown that an ensemble of the complex loops, prepared in different possible ways, is equivalent to the ensemble of cactuslike graphs where the leaves of these cacti are simple loops. The free energy of the cactuslike graphs is calculated in the mean-field approximation. The critical condition for the collapse transition is obtained. The collapsed state of the complex loop with the density distributed over different leaves is shown to be preferable.

PACS number(s): 05.40.+j, 05.70.Fh, 36.20.Ey

I. INTRODUCTION

In this paper we extend the consideration of the statistical thermodynamic properties of a single closed polymer chain (with an excluded-volume interaction) topologically entangled with an array of immobile randomly distributed (in the xy plane) parallel (in the z direction) rods to the behavior of the complex loops. In the previous part of the work [1] (referred to hereafter as I) our consideration was restricted to simple loops only, which are defined by the projection onto the xy plane, having no points of self-intersections. We considered the thermodynamic properties of simple loops in a random array of topological obstacles, states of which are characterized by the average loop length, the average number (and its dispersion) of enclosed rods, and the spatial dispersion of the density of rods in the xy plane. We concluded that at some critical values of these parameters the disorder-induced collapse transition in the simple loop occurs. The present paper extends the method proposed in I to an arbitrary and so less restrictive initial configuration of the chain (complex loop) embedded in three-dimensional (3D) space which has the points of self-intersections on the xy projection.

We would like to pay particular attention to the investigation of the influence of the "preparation conditions" on the thermodynamic properties of the polymer loops. Under the preparation conditions we understand the initial topological state of the complex loop with respect to the randomly distributed array of parallel rods. The importance of this question and the attempts to describe it quantitatively are obvious for the following reasons.

It is well known that the elastic and swelling properties of the polymer networks and gels depend strongly on the initial topological configurations, i.e., preparation conditions of the chains in the sample. The corresponding experimental data can be found in Ref. [2], whereas Ref. [3] has been devoted to some qualitative physical explanations of this phenomenon.

The influence of the preparation conditions on the chain statistics on a quantitative level was undertaken in the framework of the model "polymer chain in a translation lattice of obstacles" [4,5]. Apparently the case of translation lattice seems in some sense to be a degenerate one because the presence of random disorder in the spatial distribution of the topological constraints changes the chain statistics dramatically (see I).

Two basic conclusions will be formulated in the present paper.

(i) An arbitrary complex loop in a quenched array of topological obstacles can be represented in the form of a cactuslike type where the leaves of these cacti are the simple loops containing no points of self-intersections on the projection onto the xy plane. The points which fasten the different simple loops play the role of self-intersections.

(ii) The collapse transition of the complex loop with the fixed preparation conditions can occur independently of different "leaves" when the chain length is increased, whereas the simultaneous collapse of all leaves together is entropically unfavorable.

The main features of the theoretical methods used here have been proposed in I and represent themselves as the combination of the field-theoretic effective potential treatment [6] with replica approach [7]. The instability with respect to collapse transition in the different leaves can be described in a self-consistent way by a so-called asymmetric solution corresponding to the simplest (Gaussian) trial function with a variational parameter. This method corresponds to the well-known Feynman variational principle [8].

The paper is organized as follows. In Sec. II we describe the construction of the cactuslike representation for the complex loops starting from the simple one treated in I. The field-theoretic approach is elaborated in detail in Sec. III. The variational principle is suggested in Sec. IV, where symmetric and asymmetric solutions are analyzed in parallel.

II. CACTUSLIKE REPRESENTATION OF THE COMPLEX LOOP

Let us consider an arbitrary polymer loop embedded in 3D space and topologically entangled with an array of immobile randomly distributed rods which are placed normal to the xy plane (see Fig. 1). We assume that the loop does not produce any entanglements by itself, so its 2D xy projection gives exhaustive information about its topological state with respect to the rods. This state is the only one that is assumed to matter. To account for more general situations, such as initially knotted loops, that are thrown on the array of obstacles requires a more sophisticated analysis, which blurs the main essential results derived below.

Let us neglect for a moment the possibility of topological constraints and only pay attention to the so-called shadow graph, which is the projection of the closed chain onto the xy plane. Let us now make the reasonable assumption that this graph represents a general situation, i.e., it contains double points of path self-intersection only. An arbitrary shadow graph (corresponding to the complex loop) can be represented in the form of equivalent cactuslike graphs where each leaf has no points of self-intersections.

This correspondence is in general not unique, as can be seen from the following example: one shadow graph can be represented by several different cactuslike graphs (see Fig. 2). In Fig. 2 we show different ways of representing one shadow graph [Fig. 2(a)] by two cactuslike graphs [Figs. 2(b) and 2(c)]. The different non-self-intersecting leaves of the cactus are shaded. It is necessary to distinguish two kinds of points in cactuslike graphs. One sort of point joins different leaves of the cactus and will be called a junction point. Such points in Figs. 2(b) and 2(c) are marked with bold circles [points 1, 2, and 3 in Fig. 2(b) and points 1, 4, and 5 in Fig. 2(c)]. The second type of point occurs as a result of overlapping of the different leaves. We call them regular points [points 4 and 5 in Fig. 2(b) and points 2 and 3 in Fig. 2(c)].

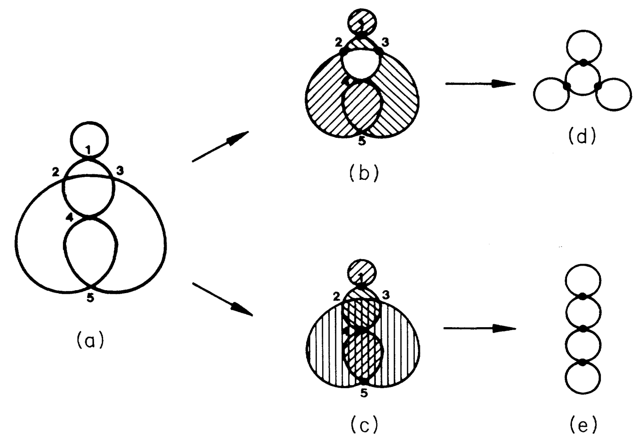

FIG. 2. A shadow graph (a); two types of its cactuslike representation (b) and (c); (d) and (e) are topological types corresponding to (b) and (c).

These differences of the covering of the shadow graph actually correspond to different ways of preparation of the initial shadow graph. The way of preparation is a succession of '"elementary technological operations" that produce a complex loop with junctions and regular points starting from a loop without self-intersections. To be more rigorous let us introduce the following definition.

Definition. We distinguish the Reidemeister moves establishing the equivalence relations of shadow link diagrams.

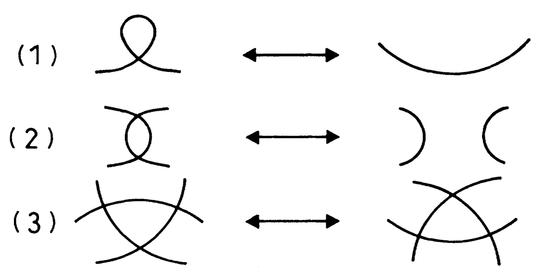

All three moves together are called ambient homotopy transformations, whereas moves (2) and (3) represent the regular homotopy transformations [9]. According to our nomenclature above the crossing point in move (1) is called a junction point; the crossing points in moves (2) and (3) are called regular points.

The contents of this section can be summarized in the following statement.

Statement. The regular way of preparation of an arbitrary shadow graph corresponding to the complex loop is as follows:

(1) We start from the simple loop and create the necessary number of junction points by means of move (1).

(2) We deform continuously the resulting cactuslike graph employing moves (2) and (3), keeping the number of junction points fixed.

(3) We sum over all different cactuslike graphs leading

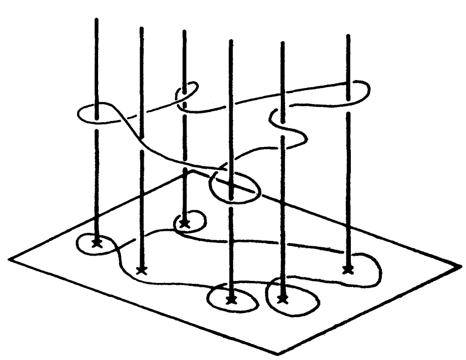

FIG. 1. The example of a complex loop (and its 2D projection) entangled with a random array of topological obstacles.

to the given complex loop.

Assumption. We suggest the probability distribution of formation of different cactuslike graphs to be uniform. Only in this case is the fraction of the shadow graphs in the ensemble increased exactly proportional to the number of covering it with cactuslike graphs. For example, the fraction of the shadow graph in Fig. 2(a) is increased twofold as a result of two types of its cactuslike coverings (or representations). So, this assumption gives us a possibility to determine the one-to-one correspondence between the ensembles of all shadow graphs and all cactuslike graphs. Otherwise (for nonuniform probability distribution) it would be necessary to discriminate the fraction of the different cactuslike graphs [e.g., Figs. 2(d) and 2(e)], which makes calculation much more complicated but does not change the main conclusion of this paper. Let us stress that this probability distribution has nothing in common with the actual statistical weight of cactuslike graphs, which results from configurational partition function of a graph with fixed number of junction points.

The real form of this probability distribution is a problem of preparation conditions of the complex loop system and is considered here as a given information (see the end of Sec. IV). Nevertheless, it seems to us natural that at the "random preparation" all different cactuslike species have the same fraction in the ensemble.

Finally, we emphasize that (in principle) the different preparation conditions could correspond to the cactuslike graphs of the same topology (see, for instance, Fig. 3). From the topological point of view the graphs in Figs. 3(b) and 3(c) are identical; they both should contribute to the shadow graph [Fig. 3(a)]. To distinguish these equivalent graphs we have to define from the very beginning the orientation (i.e., the direction of the pathway) on the shadow graph. Hence the topological charge of a simple loop (or leaf) can be both positive and negative (as has been used in I).

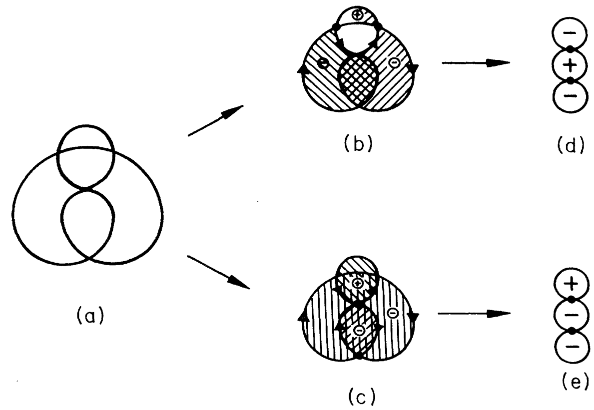

FIG. 3. Twofold [(b) and (c)] cactuslike representations of the same shadow graph (a); (d) and (e) are topologically equivalent to each other but have a different distribution of topological charges.

III. EFFECTIVE HAMILTONIAN AND MEAN-FIELD FREE ENERGY OF THE CACTUSLIKE SYSTEM

A. Field-theoretic representation of the model

In the preceding section we showed that an ensemble of randomly prepared shadow graphs coincides with an ensemble of cactuslike graphs. Let us recall the Hamiltonian from I, where we considered a simple polymer loop without self-intersections in a quenched array of topological obstacles. The replicated Hamiltonians that describes this particular system is of the following form (see also Ref. [10]):

$$H^{(n)}(\Psi,\Psi^*,\mathbf{A},g)=\sum_{\alpha=1}^{n}\psi_\alpha\left[\frac{l^2}{4}(\nabla_\perp-ig\,\mathbf{A})^2+\frac{l^2}{2}\nabla_\parallel^2+\tau\right]\psi_\alpha+\frac{La^2}{4}\sum_{\alpha=1}^{n}(\psi_\alpha\psi_\alpha^*)^2+\frac{1}{2\varphi_0}(\nabla\times\mathbf{A})^2\ , \tag{1}$$

where $\Psi=\{\psi_1,\ldots,\psi_n\}$ and $\Psi^*=\{\psi_1,\ldots,\psi_n\}$, τ is the chemical potential conjugate to the chain length, l is the length of loop segment, and L is the mean size of the coil in the z direction. The topological character of the theory is reflected in the vector potential $\mathbf{A}(r)$; g is the chemical potential conjugated to the number of obstacles enclosed by the loop (see I for more details), φ_0 is the mean density of obstacles in the xy plane. The replica index n is necessary for averaging of the free energy over the quenched disorder with simultaneous extracting of non-self-intersecting loops. The fourth-order vertex has hypercubic but not $O(n)$ symmetry because at $n\to 0$ only intrareplica interactions survived (see I).

To determine the structure of the complex loop we attribute an additional index i to the fields $\psi_{\alpha i}$ and $\psi^*_{\alpha i}$ ($i=1,\ldots,m$), which enumerates different leaves. The replica index α now counts the whole connected graph. Besides, an additional fourth-order vertex appears in the Hamiltonian, corresponding to the junction points. Thus let us introduce the Hamiltonian

$$H^{(n,m)}(\Psi,\Psi^*,\mathbf{A},g)=\sum_{\alpha=1}^{n}\sum_{i=1}^{m}\psi_{\alpha i}\left[\frac{l^2}{4}(\nabla_\perp-ig\,\mathbf{A})^2+\frac{l^2}{2}\nabla_\parallel^2+\tau\right]\psi_{\alpha i}+\frac{La^2}{4}\sum_{\alpha=1}^{n}(\psi_{\alpha i}\psi^*_{\alpha i})^2-\frac{w}{4m}\sum_{\alpha=1}^{n}\sum_{\substack{i,j\\ i\neq j}}^{m}\psi_{\alpha i}\psi^*_{\alpha i}\psi_{\alpha j}\psi^*_{\alpha j}+\frac{1}{2\varphi_0}(\nabla\times\mathbf{A})^2\ , \tag{2}$$

where τ is the mass term, i.e., here the chemical potential conjugate to the length of the whole connected graph, w is the fugacity corresponding to the number of junction points; l, L, and φ_0 are defined above.

The roman indices which enumerate the different leaves are allocated in such a way that the first fourth-order term in Eq. (2) corresponds to the 2D repulsion of excluded-volume type inside a simple loop (as in I); whereas the second fourth-order term fastens together only the different simple loops. The greek indices are attributed now to the whole connected graph.

The partition function corresponding to the Hamiltonian (2) is given by

$$Z^{(n,m)}=\exp\{-F^{(n,m)}\}=\int D\,\mathbf{A}\,D\psi_{\alpha i}D\psi^*_{\alpha i}\exp\{-H[\psi_{\alpha i};\psi^*_{\alpha i},\mathbf{A}]\}\ , \tag{3}$$

where the generating function of the connected graphs (free energy) has the form

$$F^{(n,m)}(\tau,w)=n\sum_{k=1}^{m}\sum_{p=1}^{\infty}C_m^k\mathfrak{B}(k;p)\left[-\frac{w}{m}\right]^p\ , \tag{4}$$

where $\mathfrak{B}(k;p)$ is a contribution of a connected graph constructed from k simple loops with p junction points and the combinatorial factor C_m^k gives the number of ways in which such contribution can be accomplished.

It is easy to see from the general expression Eq. (4) that the limit $m\to\infty$ corresponds to the cactuslike graphs with $p=k-1$ which are surviving. As a result the free energy of the quenched cactuslike system is given by

$$F_{\text{cactus}}=\lim_{n\to 0}\lim_{m\to\infty}\frac{1}{m}\frac{\partial}{\partial n}Z^{(n,m)}=\sum_{k=1}^{\infty}\mathfrak{B}(k;k-1)\frac{(-w)^{k-1}}{k!}\ , \tag{5}$$

where the factor $k!$ has its reason for the indistinguishable junction points and the condition $mn\to 0$ is preserved.

B. Effective free energy

Now we are in a position to do the same calculations as in I. Namely, after integration in Eq. (4) over the vector potential $\mathbf{A}$, we can write the effective free energy in the mean-field approximation with respect to ψ fields as follows:

$$\begin{aligned}F^{(n,m)}(\tau,w)=&\frac{La^2}{4}\sum_{\alpha=1}^{n}(\psi_{\alpha i}\psi^*_{\alpha i})^2-\frac{w}{4m}\sum_{\alpha=1}^{n}\sum_{\substack{i,j\\ i\neq j}}^{m}\psi_{\alpha i}\psi^*_{\alpha i}\psi_{\alpha j}\psi^*_{\alpha j}\\&-\frac{\varphi l^2g^2}{32\pi}\left[\sum_{\alpha=1}^{n}\sum_{i=1}^{m}\psi_{\alpha i}\psi^*_{\alpha i}\right]\left\{1-\ln\left[\frac{\varphi^2l^2\overline{g}^2}{4\lambda^2}\left[\sum_{\alpha=1}^{n}\sum_{i=1}^{m}\psi_{\alpha i}\psi^*_{\alpha i}\right]\right]\right\}\\&+\tau\sum_{\alpha=1}^{n}\sum_{i=1}^{m}\psi_{\alpha i}\psi^*_{\alpha i}+B\sum_{\alpha=1}^{n}\sum_{i=1}^{m}\psi_{\alpha i}\psi^*_{\alpha i}\ ,\end{aligned} \tag{6a}$$

where

$$\overline{g}^2=\frac{1}{\Delta_c}\left[1-\frac{c_0^2}{\Delta_c}\right]\ . \tag{6b}$$

c_0 is a mean topological charge of simple loops and Δ_c stands for its dispersion. In Eq. (6) λ is a cutoff parameter appearing due to ultraviolet divergence of a resulting integral, and the "mass" renormalization counterterm B is introduced to subtract this divergence.

To this end we define the counterterm B by the condition

$$\left.\frac{\delta^2}{\delta\psi_{\alpha i}\delta\psi_{\alpha i}}F^{(n,m)}\right|_{\psi_{\alpha i}=\mu_{\alpha i};\psi^*_{\alpha i}=\mu^*_{\alpha i}}=\tau\delta_{\alpha\beta}\delta_{ij} \tag{7}$$

with an arbitrary subtraction point $\psi_{\alpha i}=\mu_{\alpha i}$, $\psi^*_{\beta j}=\mu^*_{\beta j}$. We assume this point to be symmetrical with respect to all indices,

$$\mu_{\alpha i}=\mu^*_{\alpha i}\equiv\mu\ . \tag{8}$$

Proceeding from the condition (7) we obtain the value of B and substituting this in Eq. (6). We find for the free energy

$$\begin{aligned}F^{(n,m)}(\tau,w)=&\sum_{\alpha=1}^{n}\sum_{i=1}^{m}\sum_{j=1}^{m}V_{ij}\psi_{\alpha i}\psi^*_{\alpha i}\psi_{\alpha j}\psi^*_{\alpha j}-\frac{\varphi l^2\overline{g}^2}{32\pi}\left[\sum_{\alpha=1}^{n}\sum_{i=1}^{m}\psi_{\alpha i}\psi^*_{\alpha i}\right]\ln\left[\frac{1}{mn}\left[\sum_{\alpha=1}^{n}\sum_{i=1}^{m}\psi_{\alpha i}\psi^*_{\alpha i}\right]\frac{1}{\mu^2}\right]\\&+\tau\sum_{\alpha=1}^{n}\sum_{i=1}^{m}\psi_{\alpha i}\psi^*_{\alpha i}-2\mu^2\sum_{\alpha=1}^{n}\sum_{i=1}^{m}\sum_{j=1}^{m}V_{ij}\psi_{\alpha j}\psi^*_{\alpha j}-2\mu^2\sum_{\alpha=1}^{n}\sum_{i=1}^{m}\sum_{j=1}^{m}V_{ij}\psi_{\alpha i}\psi^*_{\alpha j}\\&+\frac{\varphi l^2\overline{g}^2}{32\pi}\left[\frac{1}{mn}\sum_{\alpha=1}^{n}\sum_{\beta=1}^{n}\sum_{i=1}^{m}\sum_{j=1}^{m}\psi_{\alpha i}\psi^*_{\alpha j}+\sum_{\alpha=1}^{n}\sum_{i=1}^{m}\psi_{\alpha i}\psi^*_{\alpha i}\right]\ ,\end{aligned} \tag{9a}$$

where the fourth-order vertex has the form

$$V_{ij}=\frac{La^2}{4}\delta_{ij}-\frac{w}{4m}(1-\delta_{ij}) . \tag{9b}$$

The validity of the mean-field approximation and the role of intrareplica fluctuations were investigated in Sec. 3.2 of I. The contribution of interreplica fluctuations and—as a probable possibility—the replica symmetry breakdowns are much more involved problems and need additional investigation.

IV. VARIATIONAL PRINCIPLE

A. Basic notions

The expression (9a) for the effective free energy in the mean-field approximation is symmetric with respect to the permutations of the ψ fields in the leaves and replica spaces. On the other hand, the nontrivial structure of the fourth-order vertex (9b) in the leaf space provokes us to look for an asymmetric leaf-space solution for the condensed state.

Such a solution (symmetric in the replica space and asymmetric in the leaf space) can be presented in the form

$$\psi_{\alpha i}=\bar{\psi}+\theta_i, \quad \psi^*_{\alpha i}=\bar{\psi}+\theta_i^* , \tag{10}$$

where $\bar{\psi}$, and $\bar{\psi}^*$ are average values of the order parameters, and θ fields determine the dispersion over the leaf space

$$\sigma^2=\frac{1}{m}\sum_{i=1}^{\infty}\theta_i\theta_i^* . \tag{11}$$

Let us suggest the simplest trial function, which is of the Gaussian form for the distribution function

$$P(\theta_i,\theta_i^*)\propto\exp\left\{-\frac{1}{2\sigma^2}\theta_i\theta_i^*\right\} . \tag{12}$$

Actually, the distribution (12) can be regarded as a trial function with a variational parameter σ^2. Now we are in a position to utilize the variational principle in the following.

Let us substitute Eqs. (10) and (11) in Eq. (9), taking into account the distribution (12), and proceed with the limit $m\rightarrow\infty$ in the spirit discussed above. As a result we obtain the free energy in the asymmetric state

$$f_a(\rho_a,\sigma^2;\tau,w)=\lim_{n\rightarrow 0}\lim_{m\rightarrow\infty}\frac{1}{mn}F^{(n,m)}(\rho_a,\sigma^2) , \tag{13}$$

where $\rho=\psi\psi^*$ stands for the density in this state. The variational parameters ρ and σ^2 are the solution of the pair of coupled equations

$$\frac{\partial}{\partial\rho_a}f_a(\rho_a,\sigma^2)=0, \quad \frac{\partial}{\partial\sigma^2}f_a(\rho_a,\sigma^2)=0 . \tag{14}$$

The asymmetric solution corresponds to the case $\sigma^2>0$. Its symmetric counterpart appears in the case $\sigma^2\equiv 0$,

$$f_s(\rho_s,\sigma^2=0)=\lim_{n\rightarrow 0}\lim_{m\rightarrow\infty}\frac{1}{mn}F^{(n,m)}(\rho_s,\sigma^2=0) \tag{15}$$

and the free energy is only a function of the density. The minimization determines the density in the symmetric state ρ.

The realization of this program results in the expression for the free energy (13)

$$\begin{aligned}f_a(\rho,\sigma^2)=&\tfrac{1}{4}(La^2-w)\rho^2+\left[La^2-\frac{w}{2}\right]\sigma^2\rho+\tfrac{1}{2}\left[La^2-\frac{w}{2}\right](\sigma^2)^2\\&-\frac{\varphi l^2\bar{g}^2}{32\pi}(\rho+\sigma^2)\ln[(\rho+\sigma^2)/\mu^2]+\tau(\rho+\sigma^2)-\mu^2(La^2-w)\rho-\mu^2\left[La^2-\frac{w}{2}\right]\sigma^2\\&+\frac{\varphi l^2\bar{g}^2}{16\pi}\rho+\frac{\varphi l^2\bar{g}^2}{32\pi}\sigma^2 .\end{aligned} \tag{16}$$

Below we will consider separately two possibilities [(13) and (15)] of the thermodynamic behavior.

B. Symmetric solution

In this case $\sigma^2\equiv 0$ and the free energy has the form

$$f_s(\rho_s;\tau,w)=\tfrac{1}{4}(La^2-w_s)\rho_s^2-\frac{\varphi l^2\bar{g}^2}{32\pi}\rho_s\ln(\rho_s/\mu^2)+\tau_s^*\rho_s , \tag{17a}$$

where

$$\tau_s^*=\tau-\mu^2(La^2-w_s)+\frac{\varphi l^2\bar{g}^2}{16\pi} . \tag{17b}$$

Then the minimization with respect to ρ_s yields

$$(La^2-w_s)\rho_s=\frac{\varphi l^2\bar{g}^2}{16\pi}[\ln(\rho_s/\mu^2)+1]-2\tau_s^* . \tag{18}$$

As discussed in I this equation has one stable and one unstable equation. So the first-order order transition (loop condensation) occurs and the binodal curve is determined by the equation

$$\frac{1}{N_s^{\rm bin}}=\frac{\varphi l^2\bar{g}^2}{32\pi}\ln\left[\frac{\varphi l^2\bar{g}^2}{16\pi}\frac{L}{(La^2-w_s)\mu^2}\right] , \tag{19}$$

where $N_s^{\rm bin}$ stands for the renormalized loop length at the binodal point. We have used as in I the relation

$$N=\frac{1}{\tau^*} . \tag{20}$$

It is obvious that the symmetric solution corresponds to the case of the simple loop considered in I with the only substitution $La^2 \to La^2 - w_s$. The fugacity $w_s > 0$ (see below) and this means that $N^{\rm bin} < N^{\rm bin}$ (simple loop).

The free energy (17a) at the binodal point has the form

$$f_s^{\rm bin} = \frac{1}{4}\left[\frac{\varphi l^2 \bar{g}^2}{16\pi}\right]^2 \frac{1}{La^2 - w_s} . \tag{21}$$

As usual, the renormalized quantity $N_s^{\rm bin}$ is a function of an arbitrary subtraction point μ^2. However, a small change in μ^2 is compensated by an appropriate small change of $N_s^{\rm bin}$ and density ρ_s. This idea is the main point of the method of renormalization group [6].

C. Asymmetric solution

In this case Eqs. (14) have the form

$$\tfrac{1}{2}(La^2 - w_a)\rho_a + \left[La^2 - \frac{w_a}{2}\right]\sigma_a^2 - \frac{\varphi l^2 \bar{g}^2}{32\pi}\ln[(\rho_a + \sigma_a^2)/\mu^2] + \tau - \mu^2(La^2 - w_a) + \frac{\varphi l^2 \bar{g}^2}{32\pi} = 0 , \tag{22a}$$

$$\left[La^2 - \frac{w_a}{2}\right]\rho_a + \left[La^2 - \frac{w_a}{2}\right]\sigma_a^2 - \frac{\varphi l^2 \bar{g}^2}{32\pi}\ln[(\rho_a + \sigma_a^2)/\mu^2] + \tau - \mu^2\left[La^2 - \frac{w_a}{2}\right] + = 0 .$$

These equations can be transformed to

$$(2La^2 - w_a)\sigma_a^2 = \frac{\varphi l^2 \bar{g}^2}{16\pi}\{\ln[(\rho_a + \sigma_a^2)/\mu^2] + 1\} - 2\tau_a^* - (La^2 - w_a)\rho_a , \tag{22b}$$

where

$$La^2 \rho_a = \frac{\varphi l^2 \bar{g}^2}{16\pi} + \mu^2 w_a \tag{22c}$$

and

$$\tau_a^* = \tau - \mu^2(La^2 - w_a) + \frac{\varphi l^2 \bar{g}^2}{16\pi} . \tag{22d}$$

The analysis of these equations shows again that the nontrivial values of ρ and σ^2 appear as a result of a first-order phase transition. For the binomal curve we find

$$\frac{1}{N_a^{\rm bin}} = \frac{\varphi l^2 \bar{g}^2}{32\pi}\ln\left[\frac{\varphi l^2 \bar{g}^2}{16\pi}\frac{L}{(2La^2 - w_a)\mu^2}\right] + \tfrac{1}{2}La^2 \rho_a . \tag{23}$$

The corresponding free energy (17a) at the binodal point has the form

$$f_a^{\rm bin} = \frac{1}{4}\left[\frac{\varphi l^2 \bar{g}^2}{16\pi}\right]^2 \frac{1}{2La^2 - w_a} + \frac{1}{4}La^2 \rho_2 . \tag{24}$$

It is interesting to compare the values $N_s^{\rm bin}$ and $N_a^{\rm bin}$ [see Eqs. (19) and (23)]. To this end we have to consider the density of junction points κ as a given quantity with its value being fixed as a result of preparation.

This density κ can be expressed twofold. In the symmetric case it has the form

$$\kappa = w_s \frac{\partial f_s^{\rm bin}}{\partial w_s} = \frac{w_s}{4}\left[\frac{\varphi l^2 \bar{g}^2}{16\pi}\right]^2 \frac{1}{(La^2 - w_s)^2} , \tag{25}$$

whereas in the asymmetric case we have

$$\kappa = w_a \frac{\partial f_a^{\rm bin}}{\partial w_a} = \frac{w_a}{4}\left[\frac{\varphi l^2 \bar{g}^2}{16\pi}\right]^2 \frac{1}{(2La^2 - w_a)^2} . \tag{26}$$

The expression for the difference between $N_a^{\rm bin}$ and $N_s^{\rm bin}$ can be written straightforwardly and from Eqs. (19) and (23) we find

$$\frac{1}{N_a^{\rm bin}} - \frac{1}{N_s^{\rm bin}} = \frac{\varphi l^2 \bar{g}^2}{16\pi}\left[\ln\frac{La^2 - w_s}{2La^2 - w_a} + 1\right] + \mu^2 w_a . \tag{27}$$

For appreciation of the logarithmic term in Eq. (27) we obtain from Eqs. (25) and (26) the expressions

$$\frac{La^2 - w_s}{2La^2 - w_a} = \frac{w_s}{w_a} , \tag{28a}$$

where

$$w_s = \tfrac{1}{2}(2La^2 + X) - \sqrt{La^2 X + \tfrac{1}{4}X^2} \tag{28b}$$

and

$$w_a = \tfrac{1}{2}(4La^2 + X) - \sqrt{2La^2 X + \tfrac{1}{4}X^2} , \tag{28c}$$

$$X = \frac{1}{4\kappa}\left[\frac{\varphi l^2 \bar{g}^2}{16\pi}\right]^2 . \tag{28d}$$

We suppose that the density of junction points is rather high, so that

$$\frac{La^2 \kappa}{(\varphi_0 l^2 g^2)^2} \gg 1 . \tag{29}$$

In this region Eqs. (28b) and (28c) are transformed to

$$w_s = La^2[1 - \sqrt{(1/La^2)X}\,] , \tag{30a}$$

$$w_a = 2La^2[1 - \sqrt{(1/2La^{2)}X}\,] \tag{30b}$$

and Eq. (27) obtains the form

$$\frac{1}{N_a^{\rm bin}} - \frac{1}{N_s^{\rm bin}} \approx \frac{\varphi l^2 \bar{g}^2}{16\pi}(1 - \ln 2) + \mu^2 w_a > 0 . \tag{31}$$

Thus the resulting inequality

$$N_a^{\rm bin} < N_s^{\rm bin} < N^{\rm bin} \quad \text{(simple loop)} \tag{32}$$

yields the next conclusion.

Let us first prepare the ensemble of complex loops with a given length N_0 and mean topological charge c_0 of the simple loops (or cactus leaves) with the dispersion Δ_c and density of junction points κ; the random array of obstacles is characterized by its 2D density φ_0. We call this set (as in I, where $\kappa=0$) $\{N_0, c_0, \Delta_c, \kappa, \varphi_0\}$ the preparation conditions. If now, to grow the chain length, keeping the preparation conditions fixed, then the loop condensation occurs at $N=N_a^{\rm bin}$ and the loop thermodynamic state corresponds to the asymmetric solution.

We emphasize that the inequality (29) is crucial for the result (32). It is easy to see that in the case opposite to (29) (small density of junction points) Eqs. (22b)–(22d) result in a nonphysical solution for σ^2 ($\sigma^2<0$). This means that the asymmetric state becomes favorable at high density of junction points or, in other words, a highly entangled state. It can be seen from Eqs. (30a) and (30b) that in this region $w_s < La^2$ and $w_a < 2La^2$, so the fourth-order vertex does not change its sign and the collapse is induced by the randomly distributed obstacles.

V. CONCLUSION

This paper extends the results on simple loops without the junction points presented already in paper I to the case of complex loops which have initial junction points, remaining from the preparation. We succeeded in decomposing the complex loops into areas of simple loops, since the number of junction points is conserved. Within these simple portions the theory of I can be applied, where only excluded volume forces and the constraints from the topological charge matter. To account for complex loops a second fourth-order vertex with an opposite sign in the polymer-field Hamiltonian has been introduced. The general result of I has not been changed but the phase behavior becomes richer in the sense that limiting cases for the loop length and for the symmetric and the asymmetric solutions are found.

The next step which can be achieved in this unusual system is the deformation behavior of the loop constraint by the topological charge which can serve as an easy model for rubber elasticity for strongly entangled systems. The entanglements are represented by the rigid rods, and the polymer loop represents a test chain in the entangled ensemble. The effect of the conservation of the trapped entanglements by the topological charge, in addition to the volume exclusions, will be the subject of a subsequent paper.

ACKNOWLEDGMENT

V.G.R. would like to thank Professor E. W. Fischer for his kind invitation to the MPI für Polymerforschung, where this work has been finished.

[1] S. K. Nechaev and V. G. Rostiashvili, J. Phys. (France) II **3**, 91 (1993).
[2] R. T. Deam and S. F. Edwards, Philos. Trans. R. Soc. London Ser. A **280**, 317 (1976).
[3] G. Ferry, *Viscoelastic Properties of Polymers* (Wiley, New York, 1980).
[4] B. Goldbardt and N. Goldenfeld, Phys. Rev. A **39**, 1402 (1989); **39**, 412 (1989).
[5] M. Rubinstein and E. Helfand, J. Chem. Phys. **82**, 2477 (1985).
[6] S. Coleman and E. Weinberg, Phys. Rev. D **7**, 1888 (1973).
[7] S. F. Edwards, in *Polymer Networks,* edited by A. J. Chompff and S. Newman (Plenum, New York, 1972).
[8] R. P. Feynman and A. R. Hibbs, *Path Integrals and Quantum Mechanics* (Academic, New York, 1965).
[9] L. H. Kauffman, *Braid Group, Knot Theory and Statistical Mechanics* (World Scientific, Singapore, 1989).
[10] M. G. Brereton and S. Shah, J. Phys. A **13**, 2751 (1980).